

# Electro-deposition and characterizations of nickel coatings on the carbon–polythene composite

Qian Xu · Yong-lian Qiao · Hui-jun Liu ·  
Wei-wei Meng

Received: 23 November 2008 / Accepted: 7 June 2009 / Published online: 17 June 2009  
© Springer Science+Business Media B.V. 2009

**Abstract** Nickel coating on the carbon–polythene composite plate was prepared by electrodeposition in a nickel sulfate solution in this work. The morphology and cross-sectional microstructure of the nickel coating were examined by scanning electron microscope (SEM) and optical microscope (OM), respectively. The influence of bath temperature on the nickel deposition rate was investigated experimentally. The adhesion between the coating and the substrate was evaluated by the pull-off test. The corrosion behavior of the coating in an aqueous solution of NaCl was studied by electrochemical methods. The results showed that the nickel electrodeposition rate could reach up to  $0.68 \mu\text{m min}^{-1}$  on average under conditions of cathodic current density of  $20 \text{ mA cm}^{-2}$  and bath temperature of  $60^\circ\text{C}$ . It was confirmed that increasing the bath temperature up to  $50^\circ\text{C}$  had a positive effect on the nickel deposit rate, while an adverse effect was observed beyond  $60^\circ\text{C}$ . The adhesion strength between the nickel coating and the substrate can be more than 2.3 MPa. The corrosion potential of the bright coating in the NaCl solution was more positive than that of the dull coating, and the anodic dissolution rate of the bright coating was also far lower at the same polarization potential compared with the dull coating.

**Keywords** Nickel coating · Carbon–polythene composite · Electrodeposition · Corrosion behavior · NaCl solution

## 1 Introduction

The carbon–polythene composite has been developed quickly in recent years for applications in various fields because it has the high electrical conductivity and anti-static ability besides its excellent machinability, light weight, and the common corrosion resistance like other polymers [1–3]. However, the color of the composite is usually black due to the carbon. The composite may also suffer from oxidative deterioration in severe environmental conditions, which can reduce its service life. Fortunately, nickel and nickel-based coating on carbon–polythene composites can modify the color as metallic gray, enhance its surface conductivity and hardness, and protect it from weathering [4–6].

In past years, there were some researches about preparation of the metal coating on acrylonitrile–butadiene–styrene (ABS) composites by electroless deposition, such as copper [7], gold [8], silver [9], and nickel [10]. Lee [11] also studied the corrosion and wear–corrosion resistance of the electroless-deposited Ni–P coating on a glass fiber-reinforced plastic composite. However, few works about electroplating nickel on the carbon–polythene composite plates can be found in the literature.

The objective of this study is to electroplate the nickel coating on the surface of carbon–polythene composite plates, and characterize the surface morphology and electrochemical behavior in the NaCl aqueous solution. The adhesion between the coating and the composite substrate was also evaluated by a pull-off test.

Q. Xu (✉) · Y. Qiao · H. Liu · W. Meng  
School of Materials Science and Metallurgy, Northeastern University, 110004 Shenyang, People's Republic of China  
e-mail: qianxu201@mail.neu.edu.cn

## 2 Experimental

### 2.1 Coating deposition

The carbon–polythene composite plates were fabricated by hot-pressing from thoroughly mixed carbon and polythene powders, and were used as the electroplating substrate with a dimension of 4.0 cm × 3.0 cm × 0.1 cm. Each composite plate was roughened on the surface with a chemical etchant after being ultrasonically degreased in de-ionized water and dried in air. The composition of the roughening solution and operating conditions are shown in Table 1.

The procedure for electroplating nickel on the composite plate is illustrated in Fig. 1. A nickel plate and the roughened carbon–polythene composite plate were used as the anode and the cathode, respectively. A constant current was supplied by the RNX-305D DC power supply. A nickel sulfate solution was used as the electroplating bath, which was stirred during the deposition process. The composition of the electrolyte is given in Table 2, while the coating conditions are listed in Table 3. All chemicals used in this work were of the analytical reagent grade.

### 2.2 Coating characterization

The morphology and thickness of the nickel coating were examined by scanning electron and optical microscopy

**Table 1** The composition of roughening solution and operating conditions

Chemical	Formula	Amount (g L <sup>-1</sup> )
Sulfuric acid	H <sub>2</sub> SO <sub>4</sub>	220.8
Potassium dichromate	K <sub>2</sub> Cr <sub>2</sub> O <sub>7</sub>	5.64
De-ionized water	H <sub>2</sub> O	80
Bath temperature: room temperature, 60 °C, 70 °C		
Roughening time: 10 min, 30 min		

**Table 2** Chemical composition of the electrolyte

Chemicals	Formula	Amount (g L <sup>-1</sup> )	Purpose
Nickel sulfate	NiSO <sub>4</sub> ·6H <sub>2</sub> O	40	Ni source
Nickelous chloride	NiCl <sub>2</sub> ·6H <sub>2</sub> O	15	Anode activator
Boric acid	HBO <sub>3</sub>	10	Buffer
Saccharin	C <sub>7</sub> H <sub>5</sub> NO <sub>3</sub> S	2	Brightener

**Table 3** The electroplating operating conditions

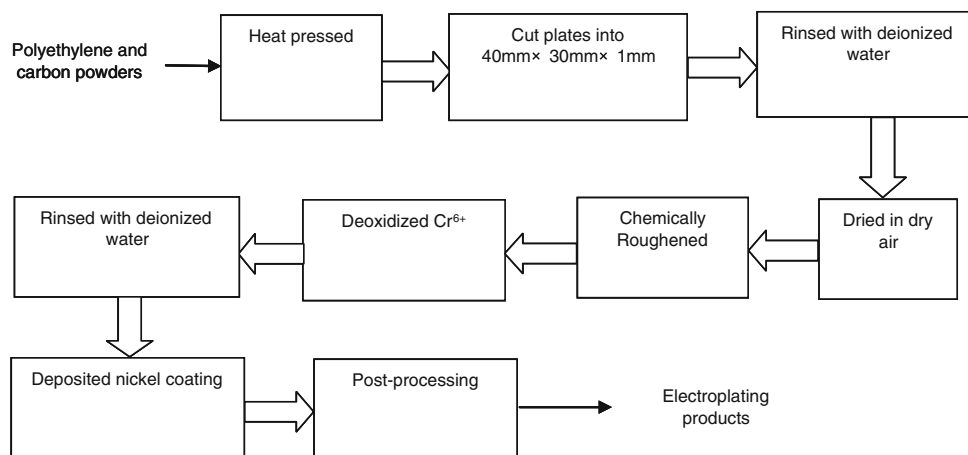
Parameters	
Bath temperature (°C)	40, 50, 60, 70
Current density (mA cm <sup>-2</sup> )	10, 15, 20, 25, 30
pH	4.7
Plating time (min)	10, 20, 30, 40, 50

(SEM and OM). The adhesion between the coating and the substrate was measured by a pull-off test with an Electronic Universal Testing Machine Model CMT5105 controlled by a computer.

### 2.3 Electrochemical measurements

Electrochemical experiments were carried out using an E.G.&G Princeton Applied Research model 2273 potentiostat in an aqueous solution of 10 wt% or saturated NaCl in the ambient environment. A conventional three-electrode cell was used. A saturated calomel electrode was used as the reference electrode, a lead plate as counter electrode, and the nickel coated plate as the working electrode which was covered by ethoxyline resin, leaving an exposed working area of 2.0 cm × 2.0 cm. Electrochemical impedance spectroscopy was performed in a frequency range between 0.1 Hz and 10 kHz, and the amplitude of the sinusoidal voltage signal was 10 mV.

**Fig. 1** The procedure for electroplating nickel on the composite plate

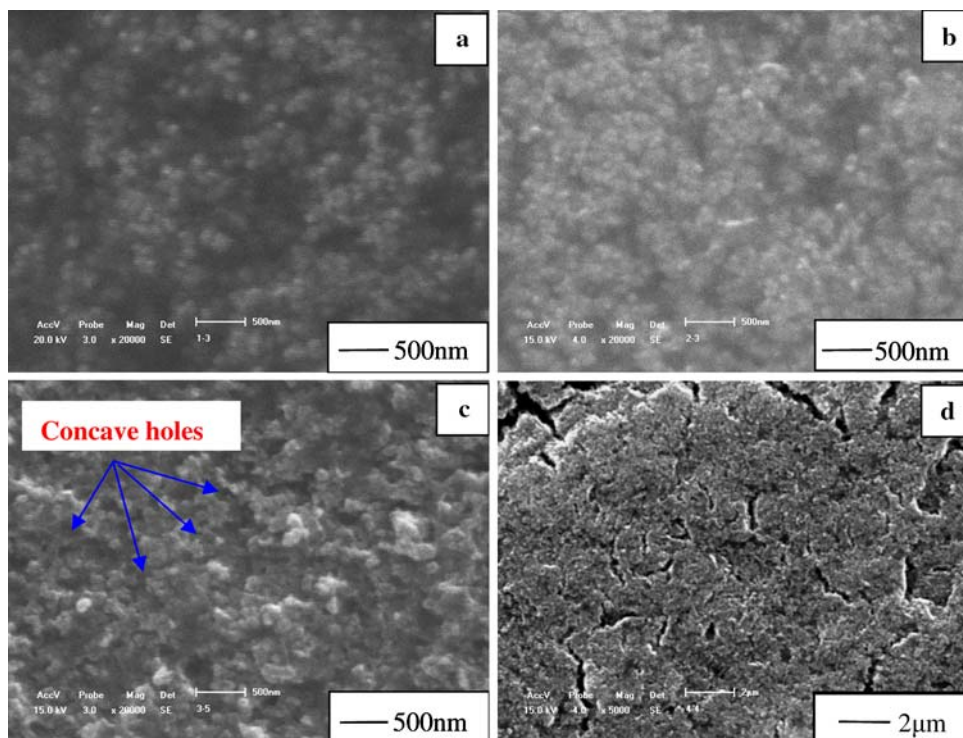


### 3 Results and discussion

#### 3.1 Roughening

The surface morphologies of the composite plate before and after roughening in various conditions are shown in Fig. 2. The results showed that the roughening temperature and the duration played important roles in the characteristics of the roughened surface. The blank composite plate (Fig. 2a) was composed of micro-grains of polythene and well-connected graphite ligaments: the latter can make the composite plate a conductor. When roughened at room temperature for 30 min, the surface morphology of the plate was not changed obviously in Fig. 2b compared with the blank plate. On the other hand, there were some concave holes on its surface when the plate was roughened at 60 °C for 10 min as shown in Fig. 2c. Most of the concave holes appeared at locations of the graphite phases, probably because of the loss of graphite through etchant corrosion. Also, the edges of the polythene micro-crystals became much sharper compared with the round ones in the blank plate. The concave holes should make it easier for the nickel particles to deposit on the plate surface and their anchor effect (or dovetail slot effect) may enhance the adhesion between the nickel coating and substrate. When roughened at 70 °C for 30 min (Fig. 2d), there were many cracks formed on the surface of the composite plate. This change could be due to the stronger attack of the etchant, leading to the disconnection of the graphite ligaments. As a

**Fig. 2** The SEM images of the composite plates with different roughening conditions. **a** without being roughened, **b** roughened at room temperature for 30 min, **c**: roughened at bath temperature of 60 °C for 10 min, **d**: roughened at bath temperature of 70 °C for 30 min



result, the conductivity of the plate decreased dramatically. Therefore, in the following discussion, all composite plates for electroplating were roughened at 60 °C for 10 min.

#### 3.2 Electrodeposition

The dependence of the nickel coating thickness on the electroplating temperature at a cathodic current density of 20 mA cm<sup>-2</sup> for 20 min is shown in Fig. 3. The OM images with a magnification of 500 for each sample are

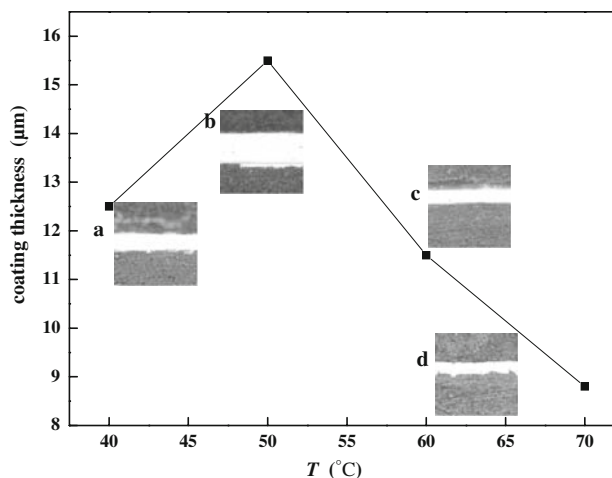


**Fig. 3** The dependence of the nickel coating thickness on the electroplating temperature. (a, b, c, and d were the OM images of the nickel coating with a magnification of 500 at the bath temperature of 40, 50, 60 and 70, respectively)

shown in the same figure. The results showed that the nickel deposition rate increased with the bath temperature rising up to 50 °C. Thereafter, the rate decreased when the bath temperature increased from 60 to 70 °C.

The electro-deposition of nickel is a process under the mixed-control [12]. The increase of the bath temperature always led to an increased ion supply toward the cathode and a decreased activation energy for the nucleation. Consequently, the deposition rate of nickel on the cathode should increase gradually as the bath temperature rises. However, during the electrodeposition of nickel on the composite plate, hydrogen evolution from the aqueous solution interferes with the plating process. Raising the temperature could make it easier for the cathodic reduction of protons, and nickel ions in the solution can precipitate as nickel hydroxide gel near the cathode [13], which could absorb the hydrogen. Both processes could suppress the nickel deposition rate on the cathode. These adverse effects on the rate of nickel deposition would be predominant and lead to the rate decreasing when the temperature was higher than 60 °C. Some bulges were observed on the nickel coating when the bath temperature was higher than 70 °C, likely because of the hydrogen gas bubbles attached to the surface. Generally, the current efficiency of the electrodeposition of Ni at 60 °C is more than 95% on average.

Figure 4 shows the SEM images of the nickel coatings formed at the cathodic current density of 25 and 20 mA cm<sup>-2</sup>, respectively. The deposition time was 20 min and the bath temperature was 60 °C in both experiments. The charge for the cathodic reduction was 3,000 C dm<sup>-2</sup> at 25 mA cm<sup>-2</sup>, and 2400 C dm<sup>-2</sup> at 20 mA cm<sup>-2</sup>. As the charge increased within the same deposition time, the grain size became larger and the grain arrangement was better structured as a consequence of the favorable nucleation and grain growth with preferred orientations.

The effect of the deposition time on the nickel coating thickness was also experimentally investigated, in which the cathodic current density was 20 mA cm<sup>-2</sup> and the bath temperature 60 °C. As shown in Fig. 5, the coating thickness increased linearly with the deposition time. Hence the

**Fig. 4** SEM images of specimen at various cathodic current densities. (**a** 25 mA cm<sup>-2</sup>, **b** 20 mA cm<sup>-2</sup>)

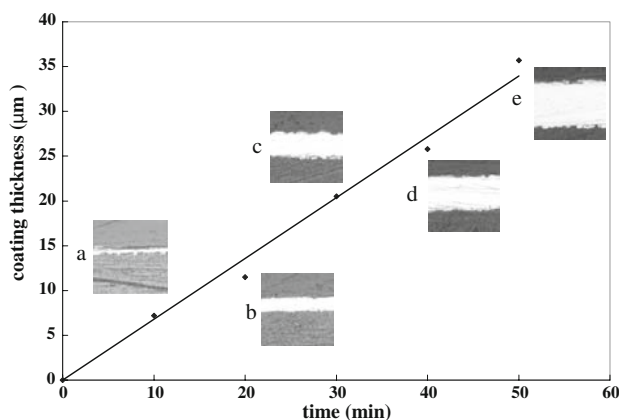
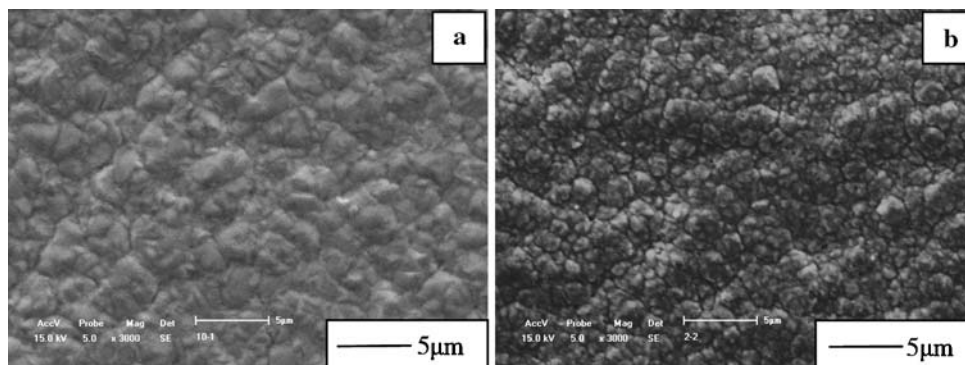


**Fig. 5** The effect of electrodeposition time on coating thickness. (*a*, *b*, *c*, *d*, and *e* were OM images of nickel coating with a magnification of 500 for the electroplating time of 10, 20, 30, 40, and 50 min, respectively)

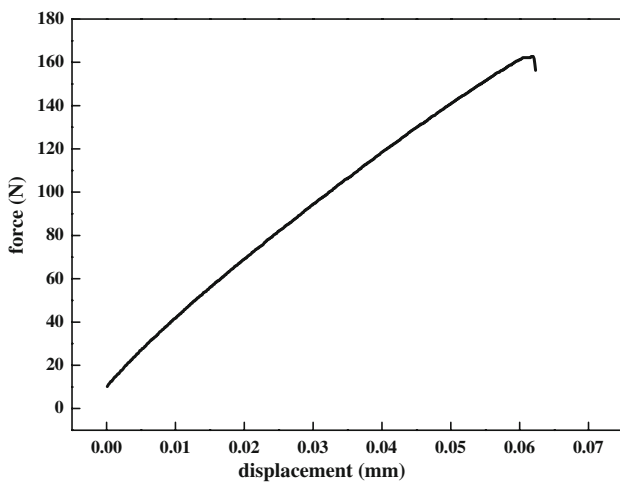
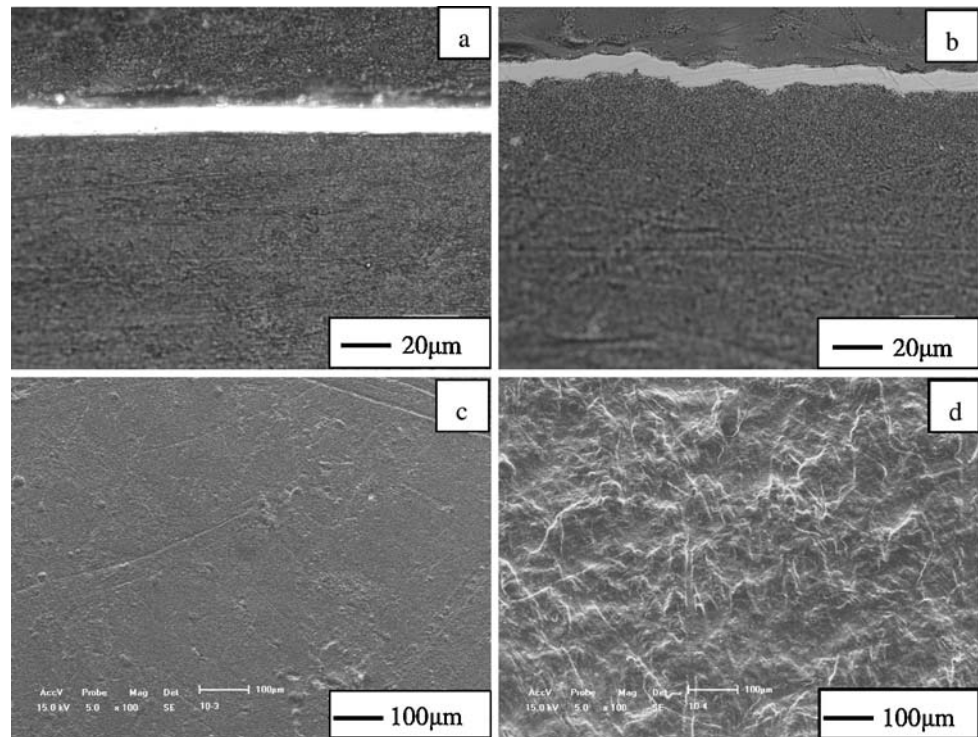
cathodic current efficiency within the deposition time of 50 min was almost constant. That means the reduction of protons on the cathode was constant and the composition in the total deposit on the cathode could be kept constant. The slope best fitted to the data in Fig. 5 gave the nickel deposition rate of 0.68 μm min<sup>-1</sup> on average.

Figure 6a and Fig. 6b show the cross-sections of the nickel coatings on the two composite plates with different roughness and morphologies as shown in Fig. 6c and Fig. 6d, respectively. The growth of nickel coatings could inherit some characteristics of the substrate geometry. Therefore, the coating roughness was strongly dependent on the roughness of the composite plate substrate. As shown in Fig. 6a and Fig. 6c, the bright coating was flatter when its substrate was much smoother. On the contrary, the dull coating was prepared on the rougher substrate shown in Fig. 6b and Fig. 6d.

### 3.3 Adhesion

The force–displacement curve for adhesion between the nickel coating and carbon–polythene composite substrate is

**Fig. 6** The cross-section OM images (a and b) of the nickel coating on carbon–polythene composite plates with different surface roughness, and their corresponding surface SEM images (c and d)



**Fig. 7** The force-displacement curve for adhesion between the nickel coating and carbon–polythene composite substrate of the pull-off test

shown in Fig. 7. The specimen was a coating composite plate which was prepared at the current density of  $20 \text{ mA cm}^{-2}$  and a bath temperature of  $60 \text{ }^\circ\text{C}$  for 50 min. One side of the plate was a bright coating and the other a dull coating. It was found that the bond between the coating and the dolly was pulled off as the maximum force of 163 N appeared on the force–displacement curve in Fig. 7. It was deduced that the pull-off adhesion strength of a coating on the plate substrate was more than 2.3 MPa since the area of the dolly bonded with the coating was  $0.7 \text{ cm}^2$ .

### 3.4 Electrochemical behavior

The electrochemical properties of the bright and dull coatings shown in Fig. 6 were studied in a saturated and a 10 wt% NaCl aqueous solutions, respectively. Figure 8 shows the potentiodynamic polarization plots of both coatings in the saturated NaCl aqueous solution. It indicates that the corrosion potential,  $E_{\text{corr}}$ , of the bright coating was about 140 mV more positive than that of the dull coating. The anodic dissolution rate of the bright coating increased more slowly with increasing the anodic overpotential as evidenced by the slope of its anodic polarization

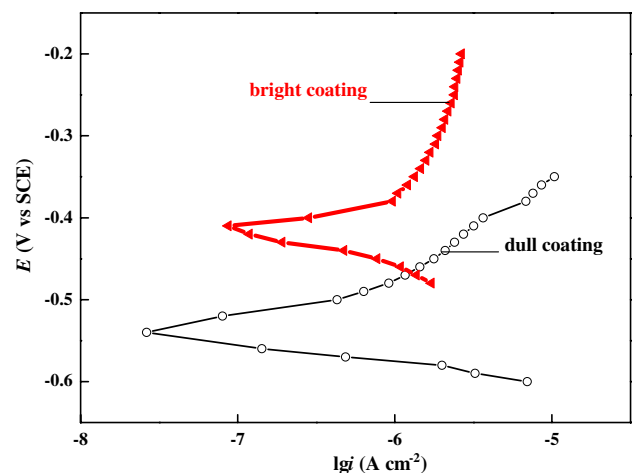
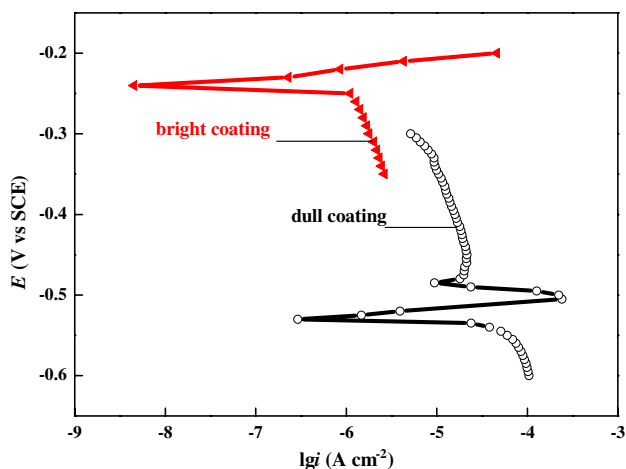


**Fig. 8** Potentiodynamic polarization plots of the bright coating and dull coating in a saturated NaCl solution

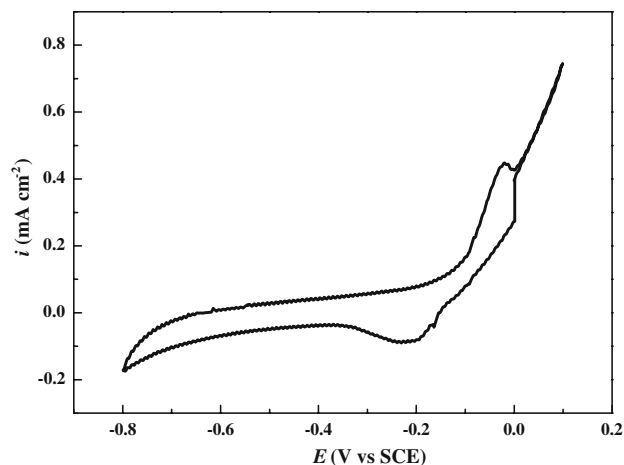
plot being larger than that of the dull coating at the potentials above  $E_{\text{corr}}$ . It was clear that the change of the surface roughness was responsible for the different results in the corrosion tests. For the surface with higher roughness, it is prone to having some inclusions and defects, which are called weak spots that could become the initial places for corrosion. The morphology of the dull coating in Fig. 6d shows that the number of crevices is much greater than that of the bright coating in Fig. 6c. The bright coating with a lower roughness had a better corrosion resistance because it had a smaller surface area which meant the corrosion reaction was slower, and the smoother surface may be easier to form the equi-potential surface for the coating which was a positive effect on the electrochemical corrosion resistance.

Figure 9 shows the polarization plots in the 10 wt % NaCl aqueous solution for the same coatings as in Fig. 8, in which the corrosion potentials of the two coatings were both shifted toward the positive direction. This indicates that 10 wt% NaCl aqueous solution was less aggressive than the saturated NaCl aqueous solution to the coatings. The passive film could have formed on the dull coating during the anodic oxidation in the 10 wt% NaCl aqueous solution, which was deduced from its polarization plot. On the contrary, there was no evidence for the dull coating to form the passive film in the saturated NaCl aqueous solution from the plots in Fig. 8. The reason should be the stronger aggression of  $\text{Cl}^-$  to the passive film at a high concentration. For the bright coating, a passive film was not found in 10 wt% NaCl aqueous solution as shown on the plot in Fig. 9, possibly because of the limitation of applied anodic potential in this study.

The cyclic voltammograms of the bright and dull coatings in the saturated NaCl aqueous solution are shown in Fig. 10 and Fig. 11, respectively. The anodic dissolution



**Fig. 9** Potentiodynamic polarization plots of the bright coating and dull coating in the 10 wt% NaCl solution



**Fig. 10** The cyclic voltammogram of the bright coating in a saturated NaCl solution

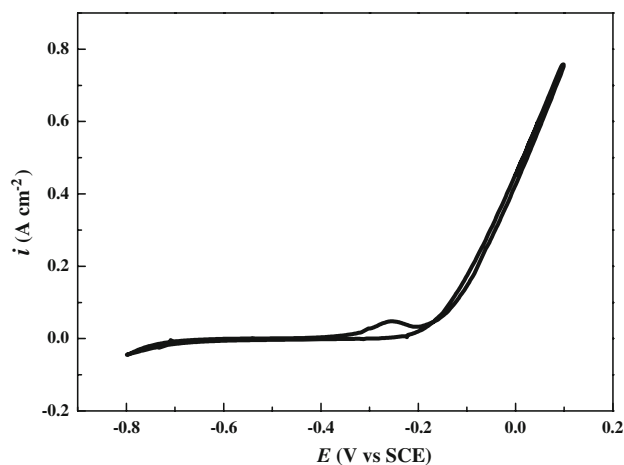


**Fig. 11** The cyclic voltammogram of the dull coating in a saturated NaCl solution

potential of the bright coating was more positive and the anodic current density far lower compared with those of the dull coating. This means the bright coating with lower roughness has higher corrosion resistance in the saturated NaCl solution, which is in agreement with the results of the potentiodynamic polarization test.

The Nyquist plots of the bright and dull coatings in the saturated NaCl aqueous solution are shown in Fig. 12. There is a distorted semicircle in the applied frequency range for each of the bright and dull coatings. The results indicate that the corrosion of the nickel coating in the saturated NaCl solution is a charge transfer-controlled process. The diameters of the distorted semicircles consist of charge transfer resistance and the oxide film resistance. The total resistances should be equal to the surface resistance value on dissolution of nickel. The surface resistance of the bright coating was about  $1.5 \times 10^4 \text{ ohm cm}^2$ , while

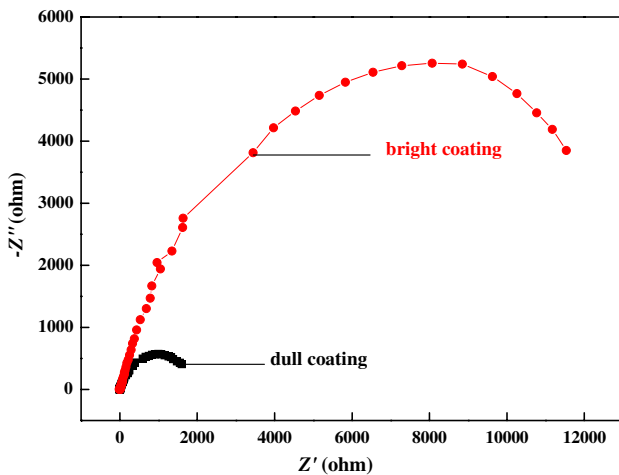


**Fig. 12** Nyquist plots of the bright and dull coatings in a saturated NaCl aqueous solution, respectively

the surface resistance of the dull coating about  $0.2 \times 10^4$  ohm  $\text{cm}^2$ . That means the bright coating had the better corrosion protection performance than the dull coating, which is in agreement with the previous deduction from the potentiodynamic polarization.

#### 4 Conclusion

- 1) It is possible to electrodeposit nickel on a carbon–polythene composite plate after the plate is roughened chemically. The coating roughness was found to be determined predominantly by the surface morphology of the composite substrate, and the adhesion strength between the coating and the substrate was more than 2.3 MPa.
- 2) The electrodeposition rate of nickel on the carbon–polythene composite plate can reach up to  $0.68 \mu\text{m min}^{-1}$  on average at a cathodic current density

of  $20 \text{ mA cm}^{-2}$  and a bath temperature of  $60 \text{ }^\circ\text{C}$ . Further increasing the bath temperature beyond  $60 \text{ }^\circ\text{C}$  had an adverse effect on the deposition rate.

- 3) The bright nickel coating with lower roughness on the carbon–polythene composite plate had better corrosion resistance in the NaCl aqueous solutions compared with the dull coating with comparatively higher roughness.

**Acknowledgments** The authors acknowledge the Natural Science Foundation of Liaoning province, China support (Grant No. 99106003). The authors are grateful to Professor Chen George Z. for critically reading the manuscript.

#### References

1. Amarasekera J (2005) *Reinf Plast*:38
2. Colbert DT (2003) *Plast Addit Compd*:18
3. Markarian J (2005) *Plast Addit Compd*:26
4. Exedra LAC, Santini MC (2005) *J Mater Process Technol* 170:37
5. Chang YY, Wang DY (2005) *Surf Coat Technol* 200:2187
6. Shen YF, Xue WY, Wang YD, Liu ZY, Zuo L (2008) *Surf Coat Technol* 202:5140
7. Kisin S, Scaltro F, Malanowski P, van der Varst PG (2007) *Polymer Degradation and Stability* 92:605
8. Yan SN, Wang YC, Wen TD, Zhu J (2006) *Phys E* 33:139
9. Dowling DP, Donnelly K, McConnell ML, Eloy R, Arnaud MN (2001) *Thin Solid Films* 398–399:602
10. Brocherieux A, Dessaux O, Goudmand P, Gengembre L, Grimblot J, Brunel M, Lazzaroni R (1995) *Appl Surf Sci* 90:47
11. Lee CK (2008) *Surf Coat Technol* 202:4868
12. Moo HS, Dong JK, Joung SK (2005) *Thin Solid Films* 489:122–129
13. Wang LP, Zhang JY, Gao Y, Xue QJ, Hua LT, Xua T (2006) *Scr Mater* 55:657